scientific reports

Check for updates

OPEN

Pharmacological activation of SERCA2 reverses ER calcium dysregulation and depression-like behaviors in hyperglycemic mice

Huiju Lee[1], Yiseul Han[1], Ju-Yeon Song[1], Do Gyeong Kim[1], Heekyoung Chung[1,2], Sung Jun Jung[1,3,5]✉ & Hyeon Son[1,4,5]✉

Chronic hyperglycemia is linked to neuronal dysfunction and mood disorders, but the underlying molecular mechanisms remain unclear. In the present study, we examined the role of sarco/endoplasmic reticulum Ca^{2+}-ATPase 2 (SERCA2) in depression-like behaviors induced by hyperglycemia, using in vivo and in vitro models. Streptozotocin (STZ)-induced hyperglycemic mice exhibited elevated glucose levels and depression-like behaviors, along with increased hippocampal endoplasmic reticulum (ER) stress markers such as C/EBP homologous protein (CHOP), neuronal loss, and reduced SERCA2 expression. Human SH-SY5Y neuroblastoma cells exposed to high-glucose (40 mM) similarly showed decreased SERCA2, elevated ER stress markers, and impaired ER calcium homeostasis. Pharmacological activation of SERCA2 by CDN1163 suppressed ER stress and reversed depression-like behaviors in STZ mice; it also restored ER calcium levels in SH-SY5Y cells. Intrahippocampal infusion of SERCA2 inhibitor thapsigargin induced ER stress and depression-like behaviors without changing SERCA2 expression, indicating that SERCA2 dysfunction alone can trigger pathology. Treatment with the ER stress inhibitor tauroursodeoxycholic acid (TUDCA) alleviated both molecular and behavioral alterations in hyperglycemic mice, supporting ER stress as a downstream effect of calcium dysregulation. These findings implicate hippocampal SERCA2 dysfunction as a central mechanism linking hyperglycemia to depression-like behaviors, highlighting SERCA2 as a potential therapeutic target.

Keywords Depression, Hyperglycemia, SERCA2, CDN1163, ER stress

Chronic hyperglycemia contributes to oxidative stress, neuroinflammation, and mitochondrial dysfunction, ultimately leading to neuronal damage and alterations in mood-regulating neurotransmitter systems[1,2]. Major depressive disorder (MDD), characterized by persistent low mood and cognitive or physical impairment[3], shows a markedly increased prevalence in diabetes, with up to threefold in type 1 and twofold in type 2 diabetes compared to the general population[4]. While traditionally considered a psychiatric condition, MDD is increasingly recognized as tightly linked to chronic physical illness, especially metabolic disorders like diabetes.

Despite this clinical association, the molecular mechanisms linking hyperglycemia to depression remain poorly understood. Streptozotocin (STZ)-induced hyperglycemia models recapitulate many diabetes-related neuropsychiatric phenotypes, including neuronal death, synaptic dysfunction, impaired neurogenesis, and hippocampal inflammation[5,6]. Pharmacological evidence suggests that metabolic regulation plays a role in mood modulation. For example, metformin has been shown to exert antidepressant-like effects through activation of AMP-activated protein kinase α (AMPKα)[7], whereas insulin—despite its essential role in the management of type 1 diabetes—has demonstrated inconsistent efficacy in neuropsychiatric outcomes[8].

One pathway through which chronic hyperglycemia may disrupt neuronal function involves intracellular calcium imbalance and endoplasmic reticulum (ER) stress[9]. The ER plays a central role in calcium homeostasis,

[1]Hanyang Biomedical Research Institute, Hanyang University, Seongdong-gu, Seoul 04763, Korea. [2]Department of Pathology, College of Medicine, Hanyang University, Seongdong-gu, Seoul 04763, Korea. [3]Department of Physiology, College of Medicine, Hanyang University, Seongdong-gu, Seoul 04763, Korea. [4]Department of Biochemistry and Molecular Biology, College of Medicine, Hanyang University, Seongdong-gu, Seoul 04763, Korea. [5]College of Medicine, Hanyang University, 222 Wangsimni-ro, Seongdong-gu, Seoul 04763, Republic of Korea. ✉email: eurijj@hanyang.ac.kr; hyeonson@hanyang.ac.kr

lipid synthesis, protein folding, and apoptosis[10]. When calcium regulation is disrupted, misfolded proteins accumulate, activating the unfolded protein response (UPR)[9]. This stress response is mediated by PKR-like endoplasmic reticulum kinase (PERK), inositol-requiring enzyme 1 α (IRE1α), and activating transcription factor 6 (ATF6). Persistent activation leads to cell death via C/EBP homologous protein (CHOP) and downstream effectors like caspase-12 and caspase-3[11,12].

A critical player in ER calcium regulation is the sarco/endoplasmic reticulum Ca^{2+}-ATPase 2 (SERCA2), which pumps cytosolic calcium into the ER lumen[13]. Dysfunction of SERCA2 leads to ER calcium depletion, followed by protein misfolding, ER stress, and apoptosis[14]. Downregulation of SERCA2 has been reported in diabetic models, particularly in peripheral tissues such as the endothelium and heart[15,16], but its role in the brain under hyperglycemic conditions remains largely unexplored.

ER stress has been implicated in both metabolic and mood disorders[17,18]. In this study, we examine the possibility that neuronal calcium dysregulation associated with ER stress provides the mechanistic link between hyperglycemia and depression, and that the calcium dysregulation is the result of reduced activity of SERCA2.

Results

STZ-induced hyperglycemia leads to depression-like behaviors in mice

To confirm depression-like behavioral alterations linked to hyperglycemia, a mouse model of STZ-induced hyperglycemia was established following previously described protocols[19,20]. Eight-week-old C57BL/6J mice were intraperitoneally (i.p.) injected with 150 mg/kg of STZ, and fasting blood glucose (FBG) was measured 3 weeks later (Fig. 1A). All mice were fasted for 6 h, and hyperglycemia was confirmed by measuring blood glucose levels in the tail vein. Mice with fasting blood glucose levels above 300 mg/dL were classified as hyperglycemic[20]. As expected, the STZ-injected mice also exhibited significantly reduced weight gain (Fig. 1B), elevated FBG (Fig. 1C), and decreased serum insulin secretion compared to vehicle controls (Fig. 1D). Levels of phosphorylated AMPKα, a well-established metabolic marker for hyperglycemia, were reduced in the hippocampi of STZ-injected mice (Fig. 1E), pointing to metabolic disturbances caused by hyperglycemia[21].

To evaluate depression-like behaviors, a battery of tests, including the female urine sniffing test (FUST), tail suspension test (TST), and open field test (OFT) was conducted. In the FUST, the time spent sniffing female urine was significantly reduced in the STZ-injected mice, indicating anhedonia-like behavior (Fig. 1F). Sniffing time for water did not differ between the groups (Fig. 1G). The STZ-injected mice exhibited significant despair-like behaviors in the TST, as evidenced by increased immobile time (Fig. 1H).

The STZ-injected mice spent less time in the center zone in the OFT (Fig. 1I), indicating increased anxiety-like behavior. Importantly, this was not due to impaired locomotion, as total distance traveled remained unchanged (Fig. 1J). Additionally, no effect on motor function was observed in the Rotarod test (Fig. 1K), confirming the absence of motor impairment. These results are consistent with previous reports that STZ-induced hyperglycemia in mice causes depression-like behavior, including anhedonia, despair, and anxiety[19].

SERCA2 reduction under hyperglycemic conditions impairs ER calcium storage and induces ER stress-related cell death

SERCA2 pumps cytosolic calcium into the ER lumen to maintain calcium stores. Its dysfunction can lead to ER calcium depletion and activation of stress responses[22]. To see whether expression of SERCA2 is reduced under hyperglycemic conditions, we measured its expression level. Molecular analyses revealed a downregulation of SERCA2 expression at both the transcriptional and translational levels in the hippocampus of STZ-treated mice, as evidenced by decreased *Atp2a2* mRNA and SERCA2 protein levels (Fig. 2A-B). At the same time, we examined the expression of ER stress markers to confirm that the reduced SERCA2 levels were associated with ER stress. Phosphorylation of IRE1α, a key sensor of ER stress, was found to be abnormally elevated (Fig. 2C). However, expression of glucose-regulated protein 78 (GRP78) was unchanged (Fig. 2D), suggesting that the adaptive chaperone response was not strongly induced. CHOP and cleaved caspase-12 have been widely used as markers of ER stress-mediated cell death[23,24]. Both proteins were markedly upregulated in the hippocampus of the STZ-injected mice (Fig. 2E), indicating that ER stress-induced cell death had been activated. The classical apoptotic markers Bax and cleaved caspase-3 were also found to be elevated (Fig. 2F). Collectively, these findings support the hypothesis that hyperglycemia is associated with reduced SERCA2 levels.

The impact of hyperglycemia on ER calcium storage was also observed using calcium imaging in SH-SY5Y cells cultured for 24 h under normal-glucose (NG, 5 mM) or high-glucose (HG, 40 mM) conditions. SH-SY5Y cells possess neuronal properties, and were chosen due to their widespread use as an in vitro model for studying calcium regulation[25]. The results confirmed that treatment of SH-SY5Y cells with high-glucose for 24 h reduced SERCA2 expression and activated ER stress and cell death pathways (Fig. S1). In addition, SH-SY5Y cells were perfused with calcium-free HEPES-buffered saline (HBS) to eliminate extracellular calcium influx and ER calcium storage was evaluated using 10 mM caffeine (CAF), which triggers calcium release from intracellular stores[26]. Under normal-glucose conditions, caffeine induced a moderate increase in cytosolic calcium, whereas this response was abolished under high-glucose conditions, indicating that ER calcium had been substantially depleted (Fig. 2G–H). To assess whether ER calcium depletion under high-glucose is due to enhanced calcium release via ER channels, we analyzed ryanodine receptors (RyR) and inositol-1,4,5-trisphosphate receptor (IP3R) isoform expressions in SH-SY5Y cells. High-glucose induced isoform-specific changes: *RYR1* and *RYR3* were downregulated, while *RYR2* remained unchanged. Among ITPR isoforms, *ITPR2* was upregulated, *ITPR3* was downregulated, and *ITPR1* was unchanged (Fig. S2). Despite preserved *RYR2* and increased *ITPR2* expression, caffeine-induced calcium release was reduced under high-glucose, suggesting that the diminished release reflects ER calcium depletion rather than altered receptor expression or function.

These findings were further validated using 2 μM thapsigargin (TG), a specific inhibitor of SERCA2. By irreversibly blocking SERCA2-mediated calcium reuptake into the ER, thapsigargin induces passive release of

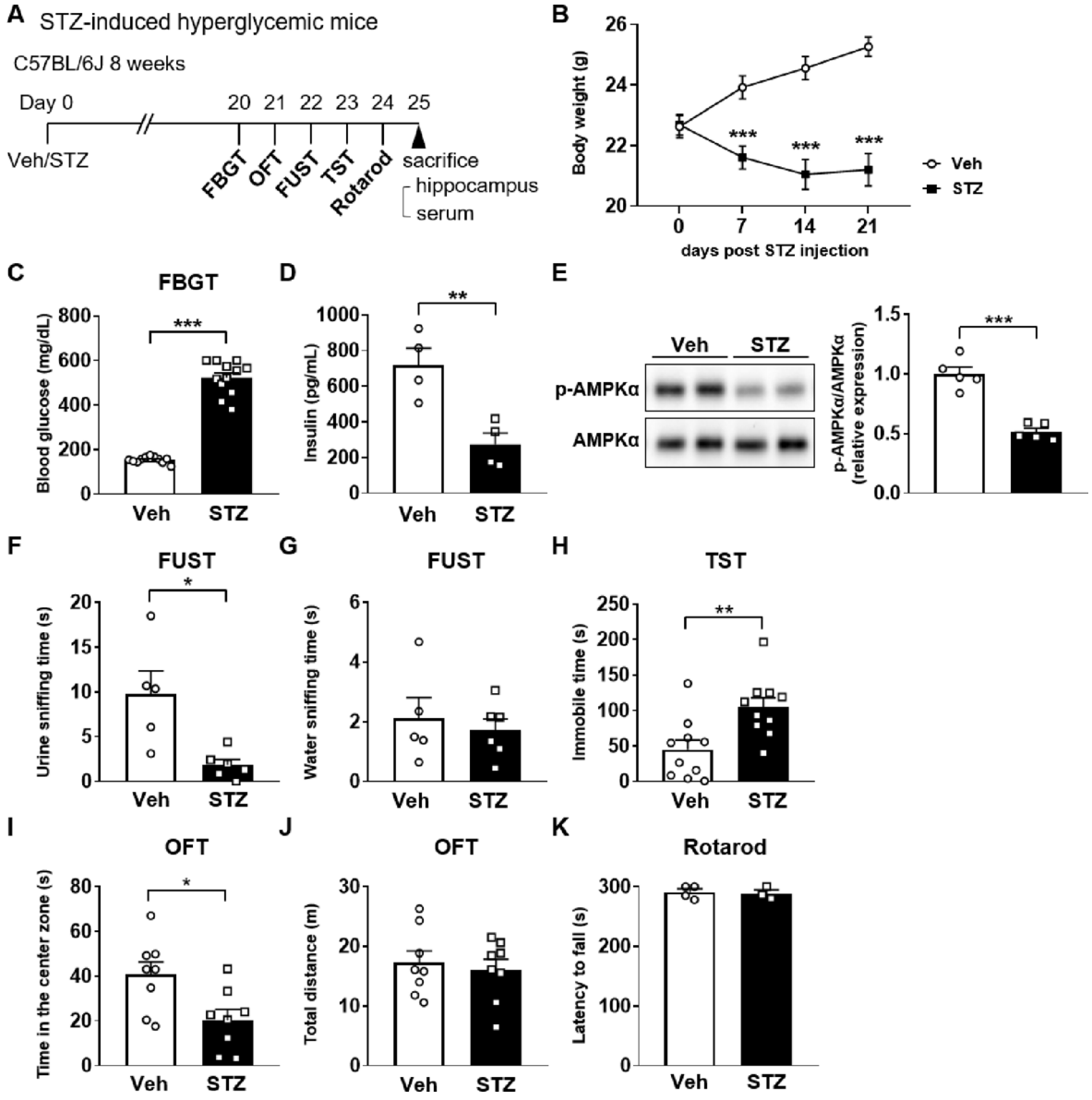

Fig. 1. STZ-injected mice exhibited hyperglycemia and depression-like behaviors. **(A)** Timeline of experimental procedures. Streptozotocin (STZ, 150 mg/kg, i.p.) was administered to induce hyperglycemia, and behavioral tests were conducted 3 weeks later. **(B)** Body weight of STZ- and vehicle-injected mice during the experimental period. **(C)** FBG levels after 6 h of fasting. **(D)** Serum insulin levels. **(E)** Phosphorylated AMPKα levels in the hippocampus. The phosphorylated form was quantified relative to the total form, and levels are shown as fold changes relative to those of the control group. Original blots are presented in Supplementary Information 2. **(F)** Female urine and **(G)** water sniffing time in the FUST. **(H)** Immobile time in the TST. **(I)** Time spent in the center zone and **(J)** total locomotor activity in the OFT. **(K)** Rotarod test for motor function. $^{*}p < 0.05$, $^{**}p < 0.01$, $^{***}p < 0.001$. All data are mean ± SEM. Detailed statistics are in Supplementary Information 1, Table S3.

stored ER calcium into the cytosol. In cells cultured under normal-glucose conditions, thapsigargin treatment in the presence of 2 mM extracellular calcium resulted in a sustained elevation of cytosolic calcium, consistent with continuous ER calcium leak due to blocked reuptake (Fig. 2I–J). In contrast, thapsigargin induced a gradual decline in cytosolic calcium levels in cells grown under high-glucose conditions, with levels at 4–6 min significantly reduced compared to the pre-thapsigargin baseline (0–2 min), suggesting compromised ER calcium retention capacity and diminished releasable calcium stores (Fig. S3A). In calcium-free conditions, thapsigargin elicited a transient cytosolic calcium increase confirming its release from ER stores (Fig. S3B-C). To further examine whether store-operated calcium entry (SOCE) contributes to the transient calcium increase, calcium imaging with 2-aminoethoxydiphenyl borate (2-APB), a SOCE modulator, revealed no significant differences between cells cultured under normal- and high-glucose conditions (Fig. S4A-B). Consistently, qPCR analysis showed no significant changes in *STIM1* or *ORAI1* mRNAs levels, key components of the SOCE pathway (Fig.

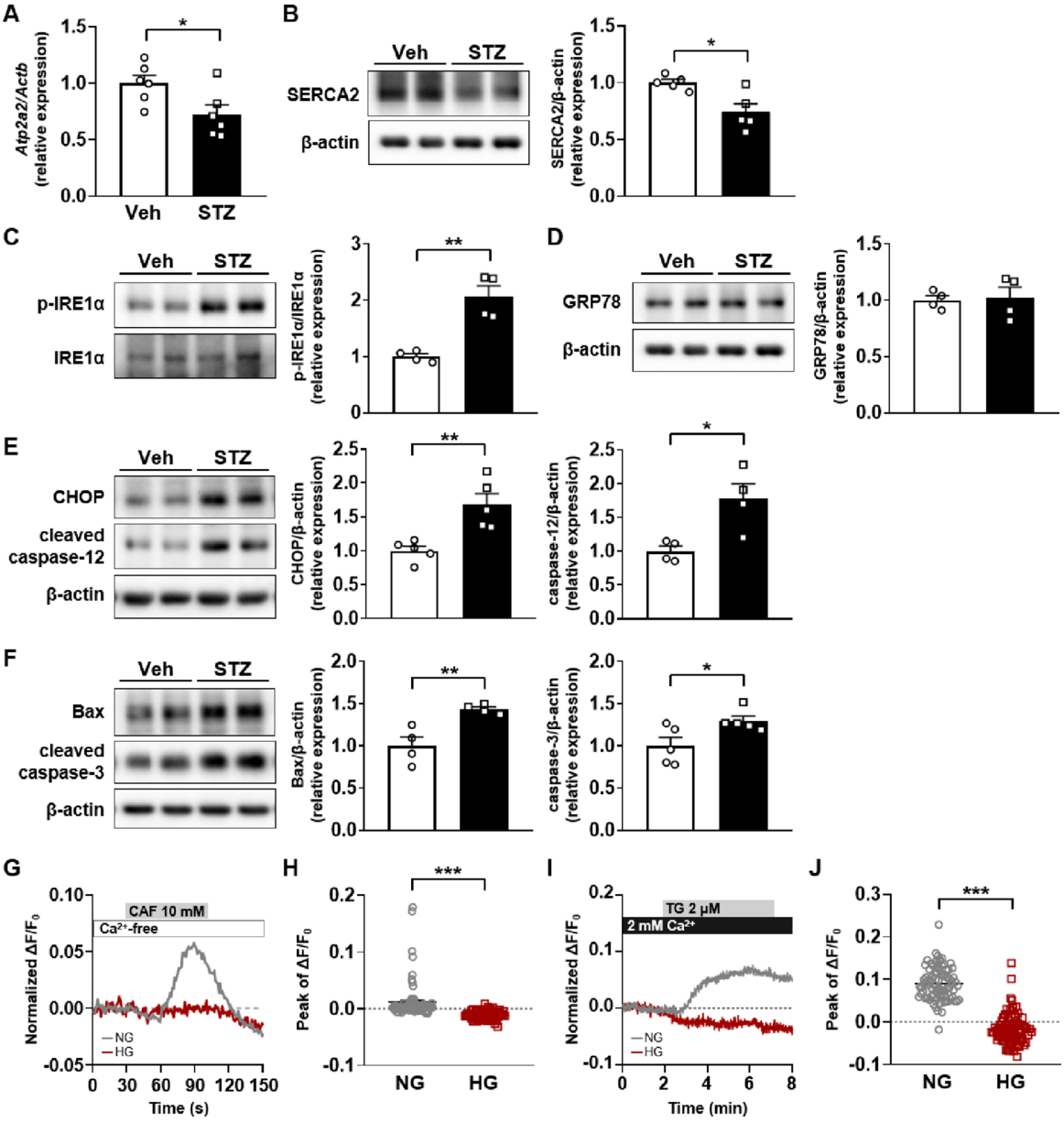

Fig. 2. Effects of hyperglycemic conditions on SERCA2 levels, ER calcium regulation, and ER stress-related cell death. **(A)** SERCA2 (denoted as *Atp2a2*) mRNA and **(B)** protein levels in the hippocampus. **(C)** Phosphorylated IRE1α levels. **(D)** GRP78 levels. **(E)** CHOP and cleaved caspase-12 levels. **(F)** Bax and cleaved caspase-3 levels. All analyses were performed in the hippocampus. Protein levels were quantified relative to β-actin or corresponding total forms, and levels are shown as fold changes relative to those of the control group. Original blots are presented in Supplementary Information 2 **(A-F)**. **(G)** Caffeine (CAF, 10 mM, 70 s) induced calcium response in SH-SY5Y cells under calcium-free conditions (NG, 5 mM, gray; HG, 40 mM, red). **(H)** Quantification of caffeine-induced calcium peak. **(I)** Thapsigargin (TG, 2 μM, 360 s) induced calcium response under 2 mM extracellular calcium conditions. **(J)** Quantification of TG-induced calcium peak. Traces were normalized to the mean fluorescence before drug perfusion **(G, I)**. NG, normal-glucose; HG, high-glucose. $^{*}p < 0.05$, $^{**}p < 0.01$, $^{***}p < 0.001$. All data are mean ± SEM. Detailed statistics are in Supplementary Information 1, Table S3.

S4C-D). These findings suggest that the cytosolic calcium increase observed following thapsigargin perfusion under high-glucose conditions is not due to enhanced SOCE activity, but rather reflects impaired SERCA2-mediated calcium reuptake and reduced ER calcium content.

SERCA2 activation alleviates depression-like behaviors by restoring ER calcium regulation under hyperglycemic conditions

Having confirmed our expectation of SERCA2 downregulation and disrupted calcium homeostasis under hyperglycemic conditions, we investigated whether the converse was also the case, namely that pharmacological activation of SERCA2 using CDN1163 could ameliorate the molecular deficits associated with hyperglycemia. CDN1163 treatment did not significantly alter SERCA2 expression (Fig. 3A), suggesting that its effects are due to functional activation of SERCA2 rather than translational upregulation, consistent with prior studies[16,27]. CDN1163 also mitigated ER stress, as evidenced by the restoration of IRE1α phosphorylation levels (Fig. 3B) and the downregulation of ER stress-mediated cell death markers, including CHOP and cleaved caspase-12 (Fig. 3C). Additionally, the elevated expression of apoptotic markers Bax and cleaved caspase-3 was attenuated by CDN1163 treatment (Fig. 3D).

To confirm that CDN1163 treatment reversed the defective ER calcium storage seen under hyperglycemic conditions, we carried out live-cell calcium imaging of SH-SY5Y cells exposed to CDN1163 under normal-glucose and high-glucose conditions. Treatment with CDN1163 produced only a modest increase in peak cytosolic calcium levels and did not markedly alter the overall calcium response dynamics in normal-glucose cells (Fig. 3E), and as anticipated treatment of high-glucose cells with CDN1163 yielded a calcium release profile similar to that of normal-glucose cells (Fig. 3E). Quantification of peak calcium responses confirmed that calcium release was significantly reduced under high-glucose conditions and restored by CDN1163 treatment (Fig. 3F-G).

To determine whether the effects of CDN1163 on ER calcium profile were due to a direct, immediate activation of SERCA2 rather than secondary downstream adaptations from chronic treatment, the compound was applied acutely during real-time calcium imaging. Acute application of CDN1163 showed minimal effect in normal-glucose cells, suggesting near-maximal basal SERCA2 activity (Fig. 3H). However, a gradual decline in cytosolic calcium was observed in high-glucose cells, indicative of partially restored ER calcium uptake (Fig. 3H). Quantitative analysis confirmed a very subtle but statistically significant difference in calcium levels between normal- and high-glucose conditions (Fig. 3I). Together, these findings demonstrate that while CDN1163 has limited effects in normal-glucose cells, it effectively restores both calcium release and uptake dynamics in high-glucose-exposed cells by rescuing impaired SERCA2 function.

Next, we investigated whether the pharmacological activation of SERCA2 using CDN1163 could ameliorate the behavioral deficits associated with hyperglycemia. CDN1163 was administered i.p. at 10 mg/kg daily for two weeks (Fig. 4A). This treatment did not alter body weight (Fig. 4B), FBG levels (Fig. 4C), or serum insulin levels compared to STZ-injected mice (Fig. 4D). CDN1163 treatment did not significantly alter hippocampal SERCA2 expression in STZ mice (Fig. 4E), consistent with results seen in SH-SY5Y cells. CDN1163 mitigated ER stress, as evidenced by the restoration of IRE1α phosphorylation levels (Fig. 4F) and the downregulation of ER stress-mediated cell death markers, including CHOP and cleaved caspase-12 (Fig. 4G). Additionally, the elevated expression of apoptotic markers Bax and cleaved caspase-3 was attenuated by CDN1163 treatment (Fig. 4H). In addition, the reduction in phosphorylated AMPKα observed in STZ-injected mice was not restored by CDN1163 treatment (Fig. 4I), indicating that the compound did not reverse systemic metabolic dysfunction. The results presented in Fig. 4J-O indicate that CDN1163 substantially alleviated the depression-like behaviors of the hyperglycemic mice, including anhedonia, despair, and anxiety. These findings collectively support the idea that high-glucose exposure compromises ER calcium storage capacity through suppression of SERCA2 function. Importantly, the restoration of ER calcium content and calcium dynamics by SERCA2 activation with CDN1163 reverses this effect, highlighting its potential as a treatment to normalize calcium homeostasis in metabolic disorders.

Intrahippocampal Inhibition of SERCA2 induces depression-like behaviors

Based on the observed reduction in SERCA2 expression under hyperglycemic conditions, we hypothesized that local inhibition of SERCA2 in the dentate gyrus (DG) might be sufficient to induce depression-like behaviors. To test this, thapsigargin (20 μM, 0.5 μl) was bilaterally infused into the DG of the hippocampus 24 h before behavioral testing (Fig. 5A-B). The DG was selected due to its role in mood regulation and vulnerability to stress-related changes[28].

In the FUST, the thapsigargin-infused mice exhibited a significant decrease in sniffing time for female urine compared to vehicle controls (Fig. 5C). Similarly, immobile time in the TST increased significantly (Fig. 5E), and in the OFT, thapsigargin-infused mice spent less time in the center zone (Fig. 5F) without any significant changes in overall locomotor activity (Fig. 5G). These results suggest that SERCA2 inhibition in the DG is sufficient to induce a depression-like behavior.

To confirm that these behavioral changes were accompanied by ER stress and cell death, molecular markers were examined 2 days post-infusion. SERCA2 expression remained unchanged (Fig. 5H) and levels of phosphorylated IRE1α were markedly increased (Fig. 5I), and CHOP and cleaved caspase-12 were upregulated (Fig. 5J). The expression of apoptotic markers, including Bax and cleaved caspase-3, was also significantly elevated (Fig. 5K).

These findings demonstrate that pharmacological inhibition of SERCA2 function in the DG of the hippocampus is sufficient to induce ER stress, activate cell death pathways, and lead to depression-like behaviors.

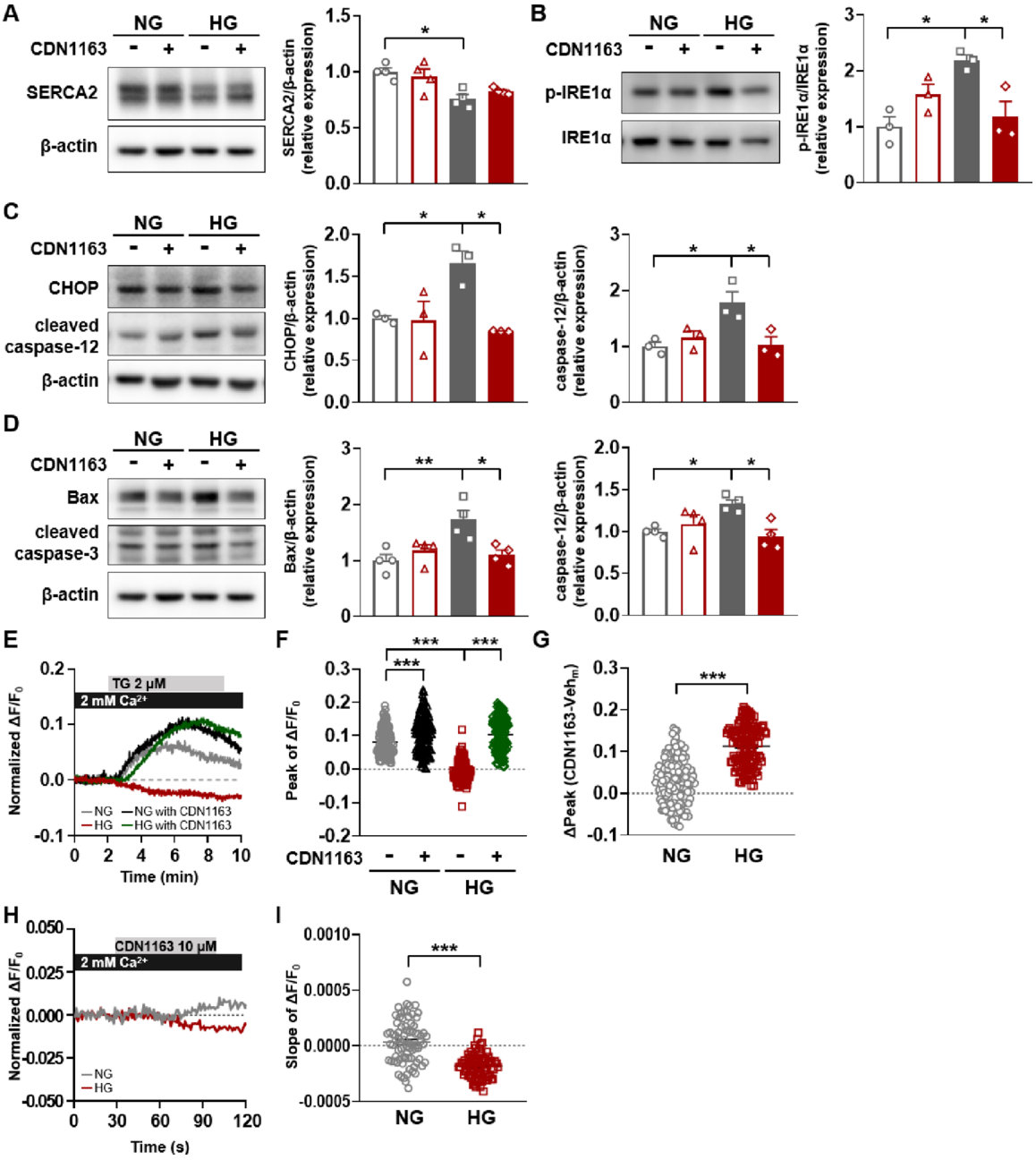

Fig. 3. SERCA2 activation by CDN1163 restores ER calcium regulation under hyperglycemic conditions in SH-SY5Y cells. **(A)** SERCA2 protein levels. **(B)** Phosphorylated IRE1α levels. **(C)** CHOP and cleaved caspase-12 levels. **(D)** Bax and cleaved caspase-3 levels. Protein levels were quantified relative to β-actin or corresponding total forms, and levels are shown as fold changes relative to those of the control group. Original blots are presented in Supplementary Information 2 **(A-D)**. **(E)** Intracellular calcium response in SH-SY5Y cells perfused with TG (2 μM, 420 s) under NG and HG conditions with or without CDN1163 (NG, gray; NG with CDN1163, black; HG, red; HG with CDN1163, green). **(F)** Quantification of TG-induced calcium peaks under 2 mM extracellular calcium conditions. **(G)** Calculation of CDN1163-induced enhancement of calcium response was performed by subtracting the mean calcium peak of the vehicle group from the calcium peak of each CDN1163-treated sample under NG and HG conditions. CDN1163 (10 μM) was co-treated under NG or HG conditions for 24 h prior to analysis **(A-G)**. **(H)** Calcium response under 2 mM extracellular calcium conditions during CDN1163 (10 μM, 70 s) treatment. **(I)** Slope of cytosolic calcium during the treatment of CDN1163. Traces were normalized to the mean fluorescence before drug perfusion **(E, H)**. $^{*}p < 0.05$, $^{**}p < 0.01$, $^{***}p < 0.001$. All data are mean ± SEM. Detailed statistics are in Supplementary Information 1, Table S3.

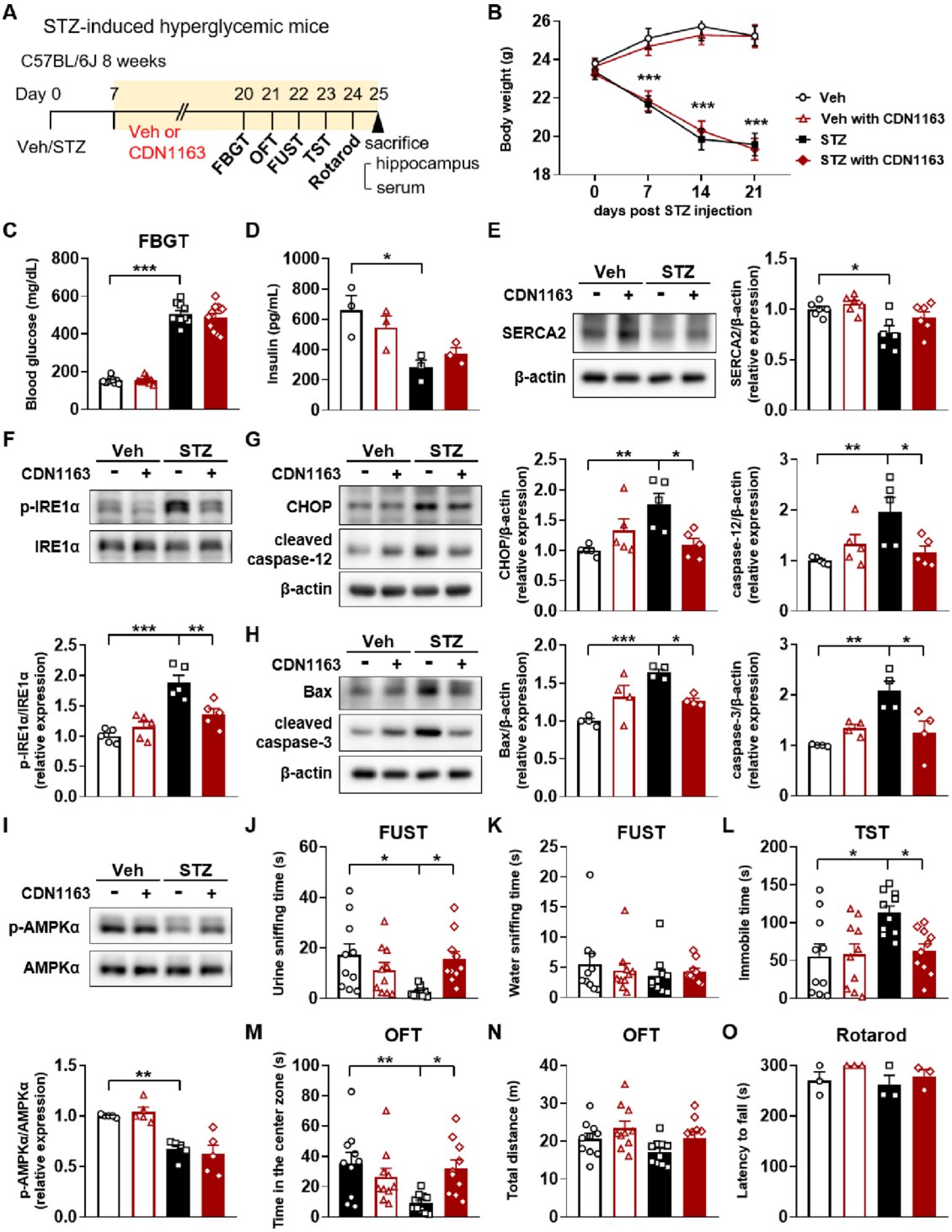

Fig. 4. SERCA2 activation by CDN1163 alleviates depression-like behaviors in STZ-induced hyperglycemic mice. **(A)** Timeline of experimental procedures. CDN1163 (10 mg/kg, i.p.) was administered once daily for 14 consecutive days before behavioral testing and continued throughout the behavioral testing period. **(B)** Body weight of vehicle- and STZ-injected mice with or without CDN1163 treatment. **(C)** FBG levels after 6 h of fasting. **(D)** Serum insulin levels. **(E)** SERCA2 levels in the hippocampus. **(F)** Phosphorylated IRE1α levels. **(G)** CHOP and cleaved caspase-12 levels. **(H)** Bax and cleaved caspase-3 levels. **(I)** Phosphorylated AMPKα levels. All analyses were performed in the hippocampus. Protein levels were quantified relative to β-actin or corresponding total forms, and levels are shown as fold changes relative to those of the control group. Original blots are presented in Supplementary Information 2 **(E-I)**. **(J)** Female urine and **(K)** water sniffing time in the FUST. **(L)** Immobile time in the TST. **(M)** Time spent in the center zone and **(N)** total locomotor activity in the OFT. **(O)** Rotarod test for motor function. $^{*}p < 0.05$, $^{**}p < 0.01$, $^{***}p < 0.001$. All data are mean ± SEM. Detailed statistics are in Supplementary Information 1, Table S3.

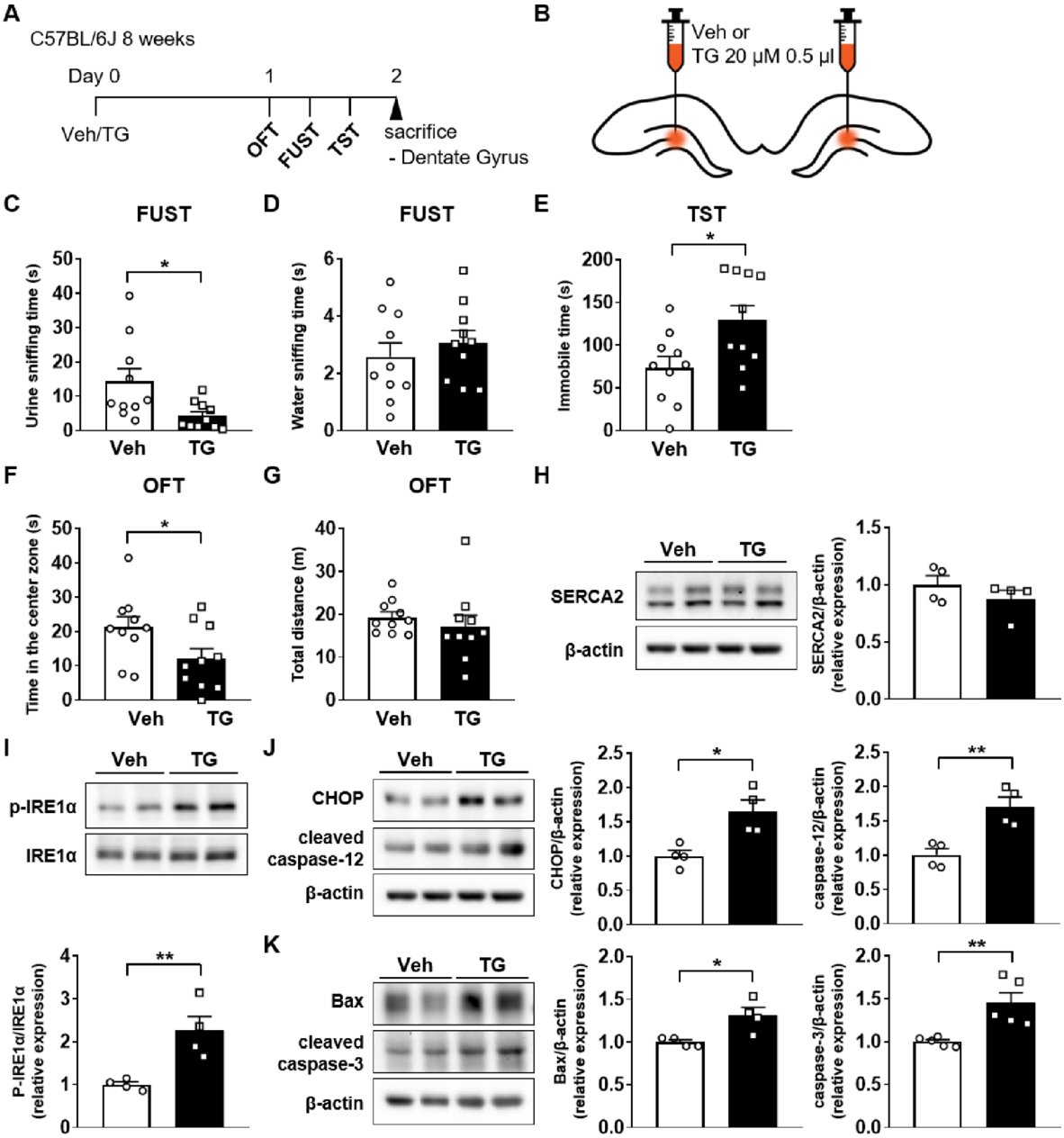

Fig. 5. Intrahippocampal inhibition of SERCA2 by thapsigargin induces depression-like behaviors. **(A)** Timeline of experimental procedures. **(B)** Microinfusions targeted to the dentate gyrus (DG) of the hippocampus. A total of 0.5 µl of 20 µM TG was injected bilaterally per side. **(C)** Female urine and **(D)** water sniffing time in the FUST. **(E)** Immobile time in the TST. **(F)** Time spent in the center zone and **(G)** total locomotor activity in the OFT. **(H)** SERCA2 expression in the DG. **(I)** Phosphorylated IRE1α levels. **(J)** CHOP and cleaved caspase-12 levels. **(K)** Bax and cleaved caspase-3 levels. All analyses were performed in the DG. Protein levels were quantified relative to β-actin or corresponding total forms, and levels are shown as fold changes relative to those of the control group. Original blots are presented in Supplementary Information 2 **(H-K)**. $^{*}p < 0.05$, $^{**}p < 0.01$, $^{***}p < 0.001$. All data are mean ± SEM. Detailed statistics are in Supplementary Information 1, Table S3.

ER stress Inhibition alleviates depression-like behaviors and cell death in hyperglycemic mice

To demonstrate directly that the inhibition of SERCA2 function seen in STZ-induced hyperglycemic mice was accompanied by ER stress, we examined the effect of tauroursodeoxycholic acid (TUDCA), a chemical chaperone and ER stress inhibitor, on STZ-induced hyperglycemic mice (Fig. 6A). TUDCA did not alter body weight (Fig. 6B) or FBG levels compared to STZ-injected mice (Fig. 6C), and serum insulin remained lower than in vehicle controls (Fig. 6D). Phosphorylated AMPKα levels were also unchanged (Fig. 6E), indicating persistent metabolic dysfunction. However, behaviorally, TUDCA significantly decreased the reduction in female urine sniffing time (Fig. 6F), whereas sniffing time for water did not differ between the groups (Fig. 6G). TUDCA

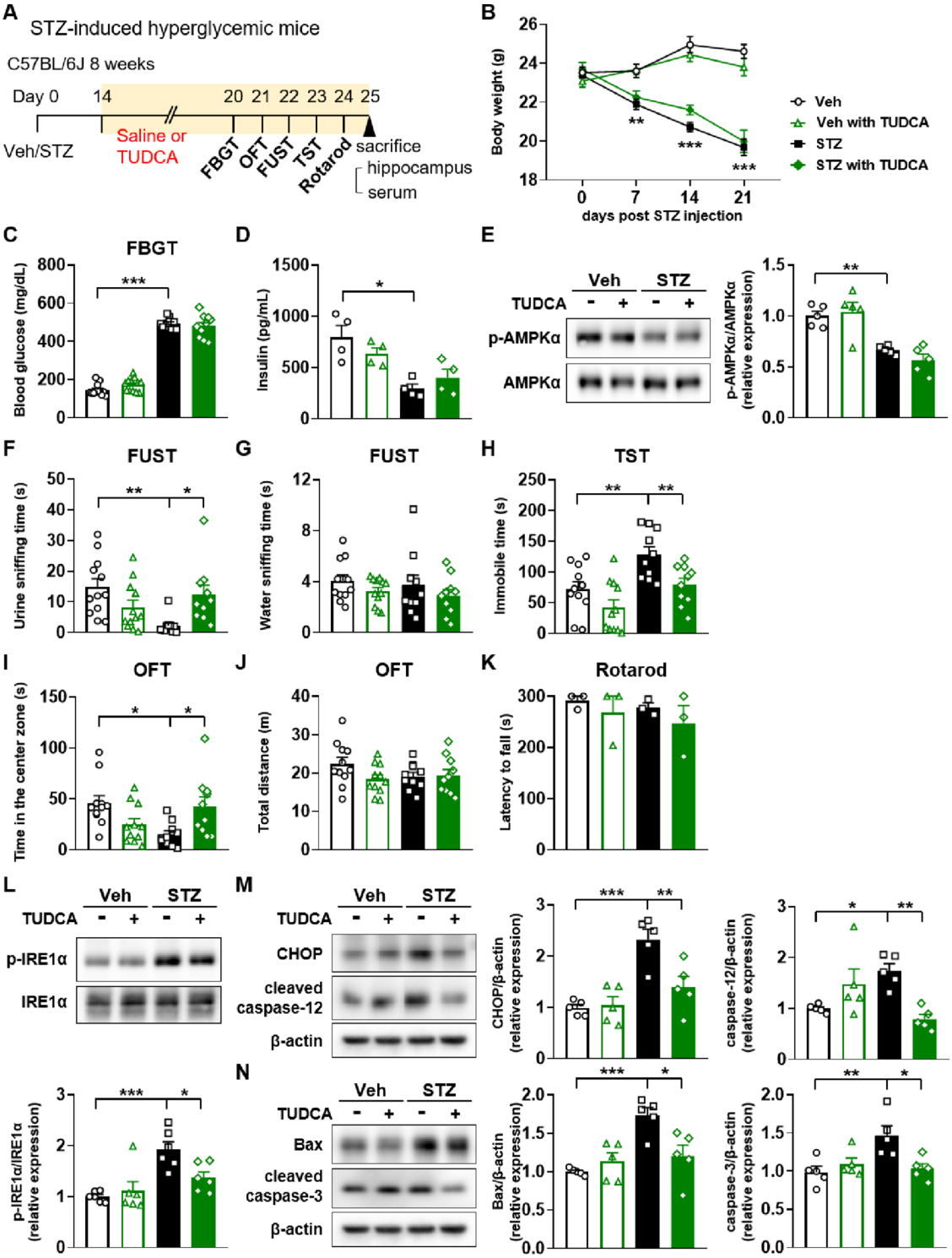

Fig. 6. ER stress inhibition by TUDCA alleviates depression-like behaviors in hyperglycemic mice. **(A)** Timeline of experimental procedures. TUDCA (300 mg/kg, i.p.) was administered once daily for 7 consecutive days before behavioral testing and continued throughout the behavioral testing period. **(B)** Body weight of vehicle- and STZ-injected mice with or without TUDCA treatment. **(C)** FBG levels after 6 h of fasting. **(D)** Serum insulin levels. **(E)** Phosphorylated AMPKα levels in the hippocampus. **(F)** Female urine and **(G)** water sniffing time in the FUST. **(H)** Immobile time in the TST. **(I)** Time spent in the center zone and **(J)** total locomotor activity in the OFT. **(K)** Rotarod test for motor function. **(L)** Phosphorylated IRE1α levels in the hippocampus. **(M)** CHOP and cleaved caspase-12 levels. **(N)** Bax and cleaved caspase-3 levels. All analyses were performed in the hippocampus. Protein levels were quantified relative to β-actin or corresponding total forms, and levels are shown as fold changes relative to those of the control group. Original blots are presented in Supplementary Information 2 **(E, L-N)**. $^{*}p < 0.05$, $^{**}p < 0.01$, $^{***}p < 0.001$. All data are mean ± SEM. Detailed statistics are in Supplementary Information 1, Table S3.

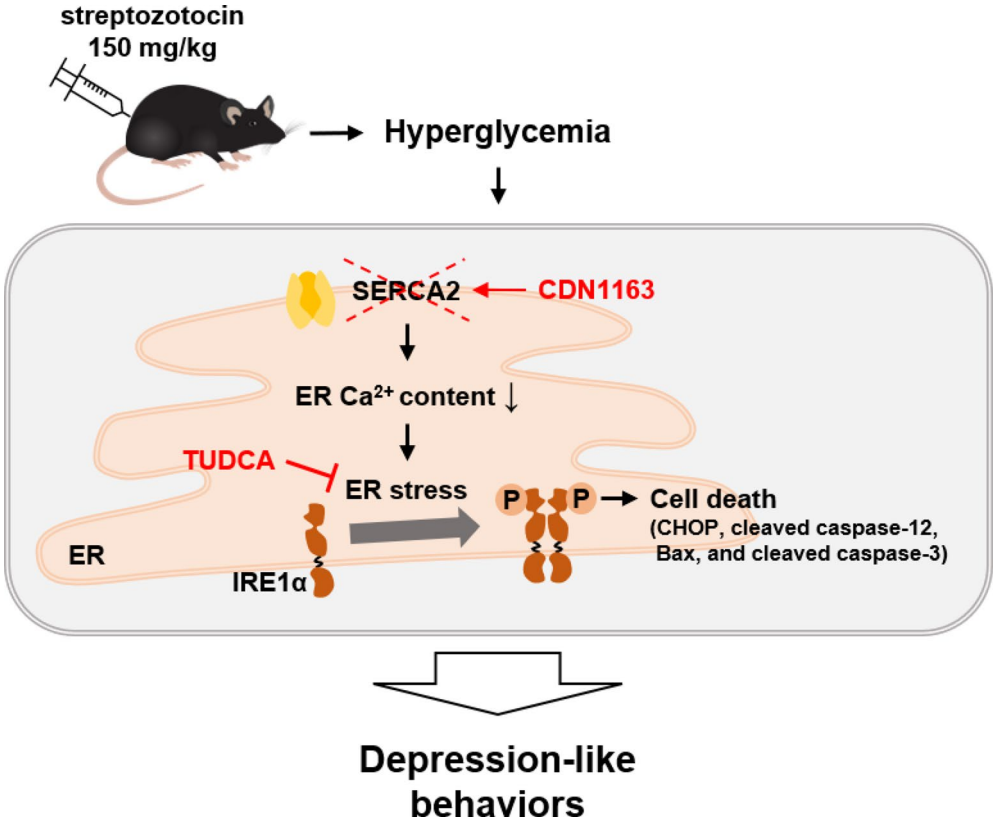

Fig. 7. Schematic diagram. Hyperglycemia induced by STZ leads to reduced expression and activity of SERCA2, resulting in impaired calcium uptake into the ER and disruption of calcium homeostasis, particularly within ER stores. This calcium imbalance elicits ER stress and activates stress response pathways such as the IRE1α signaling cascade. Persistent ER stress promotes cell death, evidenced by increased expression of CHOP and Bax together with cleavage of caspase-3 and caspase-12. These molecular alterations contribute to the development of depression-like behaviors. Treatment with TUDCA attenuates ER stress, thereby reducing cell death and ameliorating depression-like phenotypes. Pharmacological activation of SERCA2 by CDN1163 restores ER calcium regulation, which in turn alleviates ER stress, suppresses cell death, and improves behavioral outcomes.

also decreased immobile time (Fig. 6H) and increased time spent in the center zone in the OFT (Fig. 6I). No significant changes were observed in locomotor activity (Fig. 6J) or Rotarod test (Fig. 6K), indicating that motor function was not affected. TUDCA also reduced the elevated levels of phosphorylated IRE1α (Fig. 6L) and reversed the upregulation of CHOP and cleaved caspase-12 (Fig. 6M), and led to decreased expression of apoptotic markers Bax and cleaved caspase-3 (Fig. 6N). These findings confirm that the inhibition of SERCA2 function seen in STZ-induced hyperglycemic mice was accompanied by ER stress.

Discussion

Although ER stress has been implicated in both type 2 diabetes and mood disorders, the neurobehavioral consequences of ER dysfunction under hyperglycemic conditions remain insufficiently characterized. This study identifies SERCA2 dysfunction as a critical mechanistic link connecting hyperglycemia-induced ER calcium dysregulation to depression-like behaviors (*summarized in* Fig. 7). By doing so, it addresses the previously uncharacterized relationship between metabolic dysregulation and affective symptoms.

This study is, to the best of our knowledge, the first to elucidate the mechanistic connection between hyperglycemia-induced ER calcium dysregulation and depression-like behaviors, highlighting the pivotal role of SERCA2 dysfunction as follows. First, chronic treatment with SERCA2 activator CDN1163 was shown to ameliorate depression-like behaviors in a hyperglycemic mouse model, suggesting a central role for ER calcium homeostasis in mood regulation under metabolic stress. While previously studied in cardiac contexts[29], CDN1163 here demonstrated efficacy in restoring ER calcium balance within the brain, underscoring its relevance to central nervous system dysfunction. Complementary calcium imaging in neuron-like SH-SY5Y cells exposed to high-glucose conditions further confirmed that CDN1163 restores calcium handling capacity at the cellular level. Additionally, pharmacological inhibition of SERCA2 with thapsigargin reproduced key pathological features, reinforcing the causal involvement of SERCA2-mediated calcium regulation in mood-related outcomes. Furthermore, the comparable behavioral benefits observed with TUDCA, a chemical chaperone that mitigates ER stress, imply that targeting ER homeostasis may offer convergent therapeutic potential against

hyperglycemia-associated depressive phenotypes. High-glucose-treated cells showed a significant decrease in cytosolic calcium immediately after thapsigargin stimulation. This likely reflects ER calcium depletion combined with rapid mitochondrial calcium uptake[30]. The modest cytosolic change is consistent with ER stores being partially depleted under hyperglycemia, with mitochondria promptly buffering the released calcium[31,32]. These findings suggest acute ER–mitochondria cross-talk could play a role in calcium dysregulation in hyperglycemic conditions.

The SERCA family comprises three major isoforms (SERCA1-3), with tissue-specific expression patterns[33]. SERCA2 is predominantly in the brain and plays a central role in neuronal ER calcium regulation[34,35]. CDN1163 preferentially activates SERCA2a/2b isoforms[16], whereas thapsigargin irreversibly inhibits all SERCA isoforms[36]. Together with the analysis of RyR and IP3R expression under high-glucose, this contrast supports the interpretation that the observed effects are specifically attributable to SERCA2 rather than to enhanced calcium release mediated by RyR or IP3R.

Previous studies in healthy animals—in the absence of metabolic disease—reported that chronic SERCA2 activation led to behavioral impairments[37]. On the other hand, the results with CDN1163 show that it has an antidepressant-like effect in hyperglycemia. Clearly the functional impact of SERCA2 activation can vary depending on metabolic status. CDN1163 also reduced ER stress-related cell death responses (Figs. 3C-D and 4G-H), consistent with prior findings that SERCA2 activation protects neurons from damage under environmental stress conditions, such as heat exposure[38]. These results link ER calcium disruption to mood dysregulation and highlight SERCA2 as a potential therapeutic target.

Our findings suggest that, in the hippocampus of STZ-injected mice, ER dysfunction may occur and lead to cell death in the absence of compensatory GRP78, a major chaperone typically upregulated during the UPR[39]. Elevated CHOP and cleaved caspase-12, associated with IRE1α signaling[40], and general apoptotic markers such as Bax and cleaved caspase-3 support this interpretation (Fig. 2C, E-F). SERCA2 activation might reverse these changes, alleviating both ER stress and cell death, and demonstrating a metabolically independent antidepressant mechanism.

Notably, CDN1163 did not alter systemic glucose or insulin levels in STZ-injected mice (Fig. 4C-D), unlike reports in insulin-resistant models such as ob/ob or db/db mice[15,16], or the choline-deficient model of β-cell dysfunction and insulin resistance[41]. Thus, behavioral recovery by CDN1163 may occur independently of glycemic control. Similarly, in the STZ model, TUDCA treatment did not lead to improvements in metabolic parameters. This lack of effect may be attributable to the relatively short duration of treatment in our study, as previous reports have demonstrated glycemic benefits only after prolonged administration (≥ 10–15 days)[42,43]. Variations in treatment duration, dosage, and model characteristics likely account for these discrepancies, indicating that TUDCA's metabolic effects are time-dependent and merit further investigation.

While this study focused on ER dysfunction under chronic hyperglycemia, it also identifies CDN1163 as a novel therapeutic candidate for hyperglycemia-associated mood disorders. Unlike widely used antidiabetic agents such as metformin and GLP-1 receptor agonists (e.g., semaglutide/Wegovy)[7,44], which may influence brain function indirectly via systemic metabolic improvements, CDN1163 acts directly on neuronal calcium regulation by targeting ER function. Metformin has been reported to alleviate depression-like behaviors by activating AMPK signaling and reducing the hippocampal neuroinflammation, while GLP-1 analogs have shown neuroprotective effects. Thus, assessing whether these mechanisms act independently or synergistically with ER-targeted strategies like CDN1163 could inform future therapeutic designs. Although CDN1163 has shown cardioprotective effects in preclinical studies[15], potential adverse effects on the cardiovascular system cannot be excluded and warrant further investigation[45].

Building on these findings, chronic SERCA2 activation may benefit other diseases characterized by ER calcium dysregulation, including neurodegenerative and metabolic conditions. This study provides the first evidence that SERCA2 restoration reverses ER calcium dysfunction and depression-like behaviors under hyperglycemia. Continued research into the long-term, region-specific, and cell-type-specific effects of SERCA2 activation may offer novel approaches to address the clinical overlap between mood disorders and metabolic diseases.

Materials and methods

Animal preparation

Male C57BL/6J mice were group-housed (3–5/cage) under a 12-h light/dark cycle in a temperature- and humidity-controlled environment with *ad libitum* access to food and water. All animal procedures were approved by the Institutional Animal Care and Use Committee of Hanyang University. This study is reported in accordance with the ARRIVE guidelines (https://arriveguidelines.org).

Establishment and validation of STZ-induced hyperglycemic mice

Eight-week-old male mice (DBL, Korea) were i.p. injected with STZ (150 mg/kg body weight) in 50 mM citrate buffer (pH 4.5) after a 4-h fasting period. Controls received citrate buffer (Vehicle). Three weeks later, FBG was measured via tail vein after 6-h fasting using a glucometer (Accu-Chek Performa, ROCHE, Germany). Mice with FBG > 300 mg/dL were classified as hyperglycemic and used for experiments[20].

Pharmacological treatment

CDN1163 (10 mg/kg; MedChemExpress, USA) was diluted from a 100 mM DMSO stock into 10% DMSO, 40% PEG 300, 5% Tween 80, and 45% saline and given i.p. daily for 14 d. TUDCA (300 mg/kg; Millipore, USA) was dissolved in saline and administered i.p. daily for 7 d.

Insulin ELISA
Serum insulin levels were measured using a commercial ELISA kit (Morinaga, Japan; M1104). Concentrations were determined using a standard curve (0.1–6.4 ng/ml). Absorbance was read at 450 nm (reference 630 nm) with a plate reader.

Behavioral testing
Mice were habituated to the test room 1 h before behavioral tests, which were performed in random order during the dark phase. Testing apparatuses were cleaned with 70% ethanol between trials.

Female urine sniffing test
FUST was conducted in three phases: 3 min exposure to water-soaked swab, 45 min rest, then 3 min exposures to estrus female urine. Sniffing times for each stimulus were recorded[46].

Tail suspension test
Mice were suspended by the tail 45 cm above the floor using adhesive tape for 6 min. Total immobile time was recorded as the absence of limb or body movement[47].

Open field test
Mice were placed in a white plastic box (40 × 40 × 40 cm), and movements were recorded for 5 min. Time spent in the center (20 × 20 cm) and total distance moved were analyzed using EthoVision XT17 (Noldus, Netherlands)[48].

Rotarod
Motor coordination was assessed using an accelerating Rotarod (4–44 rpm over 300 s). Mice were trained for 2 d before testing. On test day, two trials were performed, and latency to fall (max 300 s) was averaged[49].

Stereotaxic surgery
Mice were anesthetized with rompun (8.5 mg/kg) and zoletil (17 mg/kg). Bilateral microinfusions of 20 μM thapsigargin (Sigma-Aldrich, USA) or saline (0.9%) in 0.1% DMSO were delivered into the dentate gyrus (-2.0 AP, ± 1.5 ML, -2.4 DV mm from bregma) using a Hamilton syringe at 0.25 μl/min for 2 min (0.5 μl per side). The Syringe remained in place for 10 min post-infusion before withdrawal. Scalp incisions were closed with wound clips.

Cell culture
SH-SY5Y cells (ATCC, VA) were maintained in DMEM with 10% FBS (Gibco, USA; 26140-079) on poly-D-lysine (20 μg/ml; Sigma-Aldrich, USA; P0899)-coated dishes at 37℃ with 5% CO_2. Cells (passages 15–30) were seeded at 2.5-3 10^4 cells/cm^2 and used the next day.

Calcium imaging
SH-SY5Y cells were loaded with 5 μM Fura-2 AM (Molecular Probes, USA) for 30 min at 37℃. Coverslips were transferred to a chamber on an inverted microscope (Olympus IX70, Japan) perfused with calcium-containing (2 mM) or calcium-free HEPES-buffered saline via a gravity-driven system (ALA-VM8, ALA Scientific Instruments, USA). Calcium-free buffer contained EGTA in place of $CaCl_2$. Caffeine (10 mM), thapsigargin (2 μM), CDN1163 (10 μM), and 2-APB (5 μM) were applied via the same system. Fluorescence at 340/380 nm was controlled using a Lambda 10-B filter wheel (Shutter Instrument, USA), and signals were recorded using an ORCA-Flash 2.8 Digital CMOS camera (Hamamatsu, Japan). Data acquisition and analysis were performed with MetaFluor® software (Molecular Devices, USA).

Western blotting
Tissues and cells were lysed with a protein extraction solution (Cell Signaling, USA; 9803). After heating with 5X SDS-PAGE buffer (Dyne Bio, Korea; 3020), proteins were loaded on 8–15% Tris-glycine gels and transferred to nitrocellulose membranes (Cytiva, USA; 10600003). Membranes were blocked in TBST with 5% BSA (Sigma-Aldrich, USA; A7906) or skim milk (BD Biosciences, USA; 232100), then incubated overnight at 4℃ with primary antibodies. A full list of antibodies is provided in Supplementary Information 1, Table S1. After washing, membranes were incubated with secondary antibodies, developed with ECL (Dyne Bio, Korea; GBE-P100), and imaged with a Gel Doc system (Bio-Rad, USA). Membranes were cut prior to antibody incubation to allow probe for proteins in different molecular weight ranges. All membrane sections originated from the same gel and were transferred under identical conditions. Cropped bands shown in the figures are derived from the full-length blots. Full-length blot images are provided in Supplementary Information 2. To quantify the blots, optical density was measured using ImageJ software (NIH, USA).

Quantitative real-time RT-PCR (qPCR)
Total RNA was extracted from tissues and cells using TRIzol™ reagent (Invitrogen, USA). Reverse transcription of 1 μg of RNA was performed using ImProm-II™ Reverse Transcriptase (Promega, USA) with oligo(dT) primers. qPCR was conducted on a CFX Connect System (Bio-Rad, USA) using a SensiFAST SYBR No-ROX mix (Meridian Bioscience, USA) according to the manufacturer's instructions. Gene expression levels were calculated using the $\Delta\Delta C_t$ method. Primer sequences are provided in the Supplementary Information 1, Table S2.

Statistical analysis

All experiments were independently repeated at least three times. Statistical analyses were performed using GraphPad Prism 8.0 (GraphPad Software, USA). Unpaired two-tailed t-tests were used for two-group comparisons; two-way ANOVA with Bonferroni's post hoc test was used when appropriate. Exact sample sizes and statistical parameters are described in Supplementary Information 1, Table S3. Data are presented as mean ± SEM. $p < 0.05$ waas considered to be statistically significant. All methods were conducted in accordance with relevant institutional guidelines and regulations.

Data availability

All relevant data are provided in the Supplementary Information.

Received: 14 July 2025; Accepted: 2 December 2025
Published online: 12 December 2025

References

1. Sandireddy, R., Yerra, V. G., Areti, A., Komirishetty, P. & Kumar, A. Neuroinflammation and oxidative stress in diabetic neuropathy: futuristic strategies based on these targets. *Int J Endocrinol* 674987 (2014).
2. Park, G. et al. Ablation of dynamin-related protein 1 promotes diabetes-induced synaptic injury in the hippocampus. *Cell. Death Dis.* **12**, 445 (2021).
3. Marx, W. et al. Major depressive disorder. *Nat. Rev. Dis. Primers*. **9**, 44 (2023).
4. Roy, T. & Lloyd, C. E. Epidemiology of depression and diabetes: a systematic review. *J. Affect. Disord.* **142**, 8–21 (2012).
5. Stranahan, A. M. et al. Diabetes impairs hippocampal function through glucocorticoid-mediated effects on new and mature neurons. *Nat. Neurosci.* **11**, 309–317 (2008).
6. Bathina, S., Srinivas, N. & Das, U. N. Streptozotocin produces oxidative stress, inflammation and decreases BDNF concentrations to induce apoptosis of RIN5F cells and type 2 diabetes mellitus in Wistar rats. *Biochem. Biophys. Res. Commun.* **486**, 406–413 (2017).
7. Ai, H., Fang, W., Hu, H., Hu, X. & Lu, W. Antidiabetic drug Metformin ameliorates Depressive-Like behavior in mice with chronic restraint stress via activation of AMP-Activated protein kinase. *Aging Dis.* **11**, 31–43 (2020).
8. Litmanovitch, E., Geva, R. & Rachmiel, M. Short and long term neuro-behavioral alterations in type 1 diabetes mellitus pediatric population. *World J. Diabetes*. **6**, 259–270 (2015).
9. Wiseman, R. L., Mesgarzadeh, J. S. & Hendershot, L. M. Reshaping Endoplasmic reticulum quality control through the unfolded protein response. *Mol. Cell.* **82**, 1477–1491 (2022).
10. Lai, E., Teodoro, T. & Volchuk, A. Endoplasmic reticulum stress: signaling the unfolded protein response. *Physiol. (Bethesda)*. **22**, 193–201 (2007).
11. Bhattarai, K. R., Riaz, T. A., Kim, H. R. & Chae, H. J. The aftermath of the interplay between the Endoplasmic reticulum stress response and redox signaling. *Exp. Mol. Med.* **53**, 151–167 (2021).
12. Mao, J., Hu, Y., Ruan, L., Ji, Y. & Lou, Z. Role of Endoplasmic reticulum stress in depression (Review). *Mol. Med. Rep.* **20**, 4774–4780 (2019).
13. Vangheluwe, P., Raeymaekers, L., Dode, L. & Wuytack, F. Modulating sarco(endo)plasmic reticulum Ca^{2+} ATPase 2 (SERCA2) activity: cell biological implications. *Cell. Calcium*. **38**, 291-302 (2005).
14. Li, K. et al. Cadmium disrupted ER Ca^{2+} homeostasis by inhibiting SERCA2 expression and activity to induce apoptosis in renal proximal tubular cells. *Int J. Mol. Sci* **24**, 5979 (2023).
15. Kimura, T. et al. Sarco/Endoplasmic reticulum Ca^{2+} ATPase 2 activator ameliorates endothelial Dysfunction; insulin resistance in diabetic mice. *Cells* **11**, 1488 (2022).
16. Kang, S. et al. Small molecular allosteric activator of the Sarco/Endoplasmic reticulum Ca^{2+}-ATPase (SERCA) attenuates diabetes and metabolic disorders. *J. Biol. Chem.* **291**, 5185–5198 (2016).
17. Hetz, C. & Saxena, S. ER stress and the unfolded protein response in neurodegeneration. *Nat. Rev. Neurol.* **13**, 477–491 (2017).
18. Ozcan, U. et al. Endoplasmic reticulum stress links obesity, insulin action, and type 2 diabetes. *Science* **306**, 457–461 (2004).
19. Baek, J. H. et al. Long-Term hyperglycemia causes depressive behaviors in mice with hypoactive glutamatergic activity in the medial prefrontal Cortex, which is not reversed by insulin treatment. *Cells* **11**, 4012 (2022).
20. Furman, B. L. Streptozotocin-Induced diabetic models in mice and rats. *Curr. Protoc.* **1**, e78 (2021).
21. Entezari, M. et al. AMPK signaling in diabetes mellitus, insulin resistance and diabetic complications: A pre-clinical and clinical investigation. *Biomed. Pharmacother.* **146**, 112563 (2022).
22. Daverkausen-Fischer, L. & Pröls, F. Regulation of calcium homeostasis and flux between the Endoplasmic reticulum and the cytosol. *J. Biol. Chem.* **298**, 102061 (2022).
23. Oyadomari, S. & Mori, M. Roles of CHOP/GADD153 in Endoplasmic reticulum stress. *Cell. Death Differ.* **11**, 381–389 (2004).
24. Nakagawa, T. et al. Caspase-12 mediates endoplasmic-reticulum-specific apoptosis and cytotoxicity by amyloid-beta. *Nature* **403**, 98–103 (2000).
25. Xicoy, H., Wieringa, B. & Martens, G. J. The SH-SY5Y cell line in parkinson's disease research: a systematic review. *Mol. Neurodegener.* **12**, 10 (2017).
26. Usachev, Y., Shmigol, A., Pronchuk, N., Kostyuk, P. & Verkhratsky, A. Caffeine-induced calcium release from internal stores in cultured rat sensory neurons. *Neuroscience* **57**, 845–859 (1993).
27. Cornea, R. L. et al. High-throughput FRET assay yields allosteric SERCA activators. *J. Biomol. Screen.* **18**, 97–107 (2013).
28. Hill, A. S., Sahay, A. & Hen, R. Increasing adult hippocampal neurogenesis is sufficient to reduce anxiety and Depression-Like behaviors. *Neuropsychopharmacology* **40**, 2368–2378 (2015).
29. Šeflová, J., Cruz-Cortés, C., Guerrero-Serna, G., Robia, S. L. & Espinoza-Fonseca, L. M. Mechanisms for cardiac calcium pump activation by its substrate and a synthetic allosteric modulator using fluorescence lifetime imaging. *PNAS Nexus*. **3**, pgad453 (2024).
30. Giorgi, C., Marchi, S. & Pinton, P. The machineries, regulation and cellular functions of mitochondrial calcium. *Nat. Rev. Mol. Cell. Biol.* **19**, 713–730 (2018).
31. Arruda, A. P. & Hotamisligil, G. S. Calcium homeostasis and organelle function in the pathogenesis of obesity and diabetes. *Cell. Metab.* **22**, 381–397 (2015).
32. Brini, M., Calì, T., Ottolini, D. & Carafoli, E. Intracellular calcium homeostasis and signaling. *Met. Ions Life Sci.* **12**, 119–168 (2013).
33. Periasamy, M. & Kalyanasundaram, A. SERCA pump isoforms: their role in calcium transport and disease. *Muscle Nerve*. **35**, 430–442 (2007).
34. Britzolaki, A., Saurine, J., Flaherty, E., Thelen, C. & Pitychoutis, P. M. The SERCA2: A gatekeeper of neuronal calcium homeostasis in the brain. *Cell. Mol. Neurobiol.* **38**, 981–994 (2018).

35. Baba-Aissa, F. et al. Distribution of the organellar Ca^{2+} transport ATPase SERCA2 isoforms in the Cat brain. *Brain Res.* **743**, 141–153 (1996).
36. Thastrup, O., Cullen, P. J., Drøbak, B. K., Hanley, M. R. & Dawson, A. P. Thapsigargin, a tumor promoter, discharges intracellular Ca^{2+} stores by specific Inhibition of the Endoplasmic reticulum Ca^{2+}-ATPase. *Proc. Natl. Acad. Sci. U S A.* **87**, 2466–2470 (1990).
37. Britzolaki, A., Cronin, C. C., Flaherty, P. R., Rufo, R. L. & Pitychoutis, P. M. Chronic but not acute Pharmacological activation of SERCA induces behavioral and neurochemical effects in male and female mice. *Behav. Brain Res.* **399**, 112984 (2021).
38. Li, H. et al. Heat stress induces calcium dyshomeostasis to subsequent cognitive impairment through ERS-mediated apoptosis via SERCA/PERK/eIF2α pathway. *Cell. Death Discov.* **10**, 280 (2024).
39. Mujumdar, N. et al. Triptolide activates unfolded protein response leading to chronic ER stress in pancreatic cancer cells. *Am. J. Physiol. Gastrointest. Liver Physiol.* **306**, G1011–1020 (2014).
40. Zhang, J. et al. Deoxynivalenol induces Endoplasmic reticulum stress-associated apoptosis via the IRE1/JNK/CHOP pathway in Porcine alveolar macrophage 3D4/21 cells. *Food Chem. Toxicol.* **180**, 114033 (2023).
41. Kong, L. et al. Trimethylamine N-oxide impairs β-cell function and glucose tolerance. *Nat. Commun.* **15**, 2526 (2024).
42. Ozcan, U. et al. Chemical chaperones reduce ER stress and restore glucose homeostasis in a mouse model of type 2 diabetes. *Science* **313**, 1137–1140 (2006).
43. Bronczek, G. A. et al. The bile acid TUDCA improves Beta-Cell mass and reduces insulin degradation in mice with Early-Stage of Type-1 diabetes. *Front. Physiol.* **10**, 561 (2019).
44. McIntyre, R. S. et al. The neuroprotective effects of GLP-1: possible treatments for cognitive deficits in individuals with mood disorders. *Behav. Brain Res.* **237**, 164–171 (2013).
45. Huang, Y. P. et al. CDN1163, a SERCA activator, causes intracellular Ca^{2+} leak, mitochondrial hyperpolarization and cell cycle arrest in mouse neuronal N2A cells. *Neurotoxicology* **98**, 9–15 (2023).
46. Meng, F. et al. Brain-derived neurotrophic factor in 5-HT neurons regulates susceptibility to depression-related behaviors induced by subchronic unpredictable stress. *J. Psychiatr Res.* **126**, 55–66 (2020).
47. Lee, E. H., Park, J. Y., Kwon, H. J. & Han, P. L. Repeated exposure with short-term behavioral stress resolves pre-existing stress-induced depressive-like behavior in mice. *Nat. Commun.* **12**, 6682 (2021).
48. Ko, S. Y. et al. Transient receptor potential melastatin 2 governs stress-induced depressive-like behaviors. *Proc. Natl. Acad. Sci. U S A.* **116**, 1770–1775 (2019).
49. Shiotsuki, H. et al. A Rotarod test for evaluation of motor skill learning. *J. Neurosci. Methods.* **189**, 180–185 (2010).

Acknowledgements

This work was supported by the National Research Foundation of Korea (NRF) grant funded by the Korean government (MSIT) (RS202516065222 to H.S. and RS202300302489 to S.J.J.).

Author contributions

H.L. designed and performed behavioral and biochemical experiments, analyzed the data, interpreted the results, and prepared the manuscript draft. Y.H. conducted calcium imaging. J.Y.S. and D.G.K. contributed to laboratory experiments. H.C. provided critical review and contributed reagents. S.J.J. interpreted the results, provided critical review and discussion, and contributed reagents. H.S. defined the research theme, designed the experiments, and wrote the paper. All authors reviewed and approved the final manuscript.

Declarations

Competing interests

The authors declare no competing interests.

Ethics statement

This research has been approved by the Institutional Animal Care and Use Committee of Hanyang University.

Additional information

Supplementary Information The online version contains supplementary material available at https://doi.org/10.1038/s41598-025-31293-7.

Correspondence and requests for materials should be addressed to S.J.J. or H.S.